(6) Koberstein, J. T. *J. Polym. Sci., Polym. Phys. Ed.* **1982**, *20*, 593.
(7) Bates, F. S.; Berney, C. V.; Cohen, R. E.; Wignall, G. D. *Polymer* **1983**, *24*, 519.
(8) Miller, J. A.; Cooper, S. L.; Han, C. C.; Pruckmayer, G. *Macromolecules* **1984**, *17*, 1063.
(9) Miller, J. A.; Pruckmayer, G.; Epperson, J. E.; Cooper, S. L. *Polymer* **1985**, *26*, 1915.
(10) Miller, J. A.; Mckenna, J. M.; Pruckmayer, G.; Epperson, J. E.; Cooper, S. L. *Macromolecules* **1985**, *18*, 1727.
(11) Hashimoto, T.; Shibayama, M.; Kawai, H. *Macromolecules* **1980**, *13*, 1237.
(12) Matsushita, Y.; Nakao, Y.; Saguchi, R.; Choshi, H.; Nagasawa, M. *Polym. J. (Tokyo)* **1986**, *18*, 493.
(13) Ohtani, H.; et al., to be submitted for publication.
(14) Glinka, C. J. *AIP Conf. Proc.* **1981**, *No. 89*, 395.
(15) Maconnachie, A. *Polymer* **1984**, *25*, 1068.
(16) Wignall, G. D.; Bates, F. S. *J. Appl. Crystallogr.* **1987**, *20*, 28.
(17) Maconnachie, A.; Richards, R. W. *Polymer* **1978**, *19*, 739.
(18) Yang, H.; Stein, R. S.; Han, C. C.; Bauer, B. J.; Kramer, E. J. *Polym. Commun.* **1986**, *27*, 132.
(19) Han, C. C.; et al., to be submitted for publication.
(20) Bates, F. S.; Wignall, G. D. *Macromolecules* **1986**, *19*, 934.
(21) de la Cruz, M. O.; Sanchez, I. C. *Macromolecules*, **1986**, *19*, 2501.
(22) Matsushita, Y.; et al., to be submitted for publication.
(23) Hashimoto, T., private communication.
(24) de Gennes, P.-G. *Scaling Concepts in Polymer Physics*; Cornell University: Ithaca, NY, 1979; Chapter 4.

Structural Studies of Semifluorinated *n*-Alkanes. 3. Synthesis and Characterization of $F(CF_2)_n(CH_2)_m(CF_2)_nF$

R. J. Twieg and J. F. Rabolt*

IBM Research, Almaden Research Center, 650 Harry Road, San Jose, California 95120-6099. *Received September 18, 1987; Revised Manuscript Received November 18, 1987*

ABSTRACT: A series of semifluorinated triblock oligomers of the form $F(CF_2)_n(CH_2)_m(CF_2)_nF$ (F*n*H*m*F*n* in our notation) have been synthesized and characterized by thermal analysis and low-frequency Raman measurements. Only a single endotherm is observed for the series of F12H*m*F12 ($6 \leq m \leq 22$) molecules corresponding to the crystalline melting point. In the limit of vanishing m, the melting point of $F(CF_2)_{24}F$ has been predicted by extrapolation and compared with that which recently appeared in the literature. Low-frequency (30–330 cm^{-1}) Raman measurements revealed the presence of two bands attributable to the longitudinal acoustical mode oscillations (LAM) of the extended molecule.

Introduction

The use of the Raman-active longitudinal acoustical mode (LAM) to characterize ordered chain extension in long-chain oligomers[1] and polymer crystalline lamellae[2] has been well established.[3] The relationship between vibrational frequency and inverse chain length has been found to hold in most cases and allows the determination of the length of an ordered chain sequence once a calibration curve has been determined. In particular, the Raman-active LAM has been useful[4-7] in the study of semiflexible diblock oligomers of the form $F(CF_2)_n(CH_2)_mH$ (referred to as F*n*H*m* in our notation). These molecules have been of particular interest because they are precursors of semiflexible polymers and, in addition, exhibit solid–solid phase transitions[7] that have been shown to be analogous to the "rotator" phase in *n*-paraffins. Previous studies[4] of these materials above their melting points using the Raman-active LAM indicated that only the *n*-alkyl part of the molecule became disordered, while the stiffer fluorocarbon portion remained rigid (provided that the number of CF_2 units was equal to or less than 12). This unique behavior of the F*n*H*m* molecules prompted the synthesis of a series of triblock materials of the form F12H*m*F12 (with $6 \leq m \leq 22$).

The preparation of linear diblock materials F*n*H*m* is generally accomplished in two steps by the addition of perfluoroalkyl iodide $F(CF_2)_nI$ to a 1-alkene C_mH_{2m} that produces an iodine-containing intermediate (F*n*H*m*I), which is subsequently dehalogenated to the final diblock compound (F*n*H*m*). The first step generally involves heating the perfluoroalkyl iodide neat with the olefin in the presence of an initiator. Many initiators and catalysts for this process have been described, but simple free radical initiators such as azobis(isobutyronitrile) (AIBN) at an elevated temperature (typically >70 °C for AIBN reactions) are very effective. The second step most often involves the reduction of the iodide intermediate with zinc in ethanolic HCl. We have found that these reaction conditions suffice for most F*n*H*m* where $n = 6$–12 and $m = 6$–20. Reactions involving perfluoroalkyl or olefin components with boiling points significantly less than 70 °C require the use of pressure vessels or flow systems.

Brace has reported the successful preparation of the triblock halogenated (F*n*H*m*F*n*I2) compounds F4H6F4I2 and F4H8F4I2 (from iodoperfluorobutane and 1,5-hexadiene and 1,7-heptadiene, respectively) under conditions essentially identical with those used for the diblock F*n*H*m*I materials.[8] The dehalogenation of these iodine-containing materials to F4H6F4 and F4H8F4 apparently has not been described. In these low molecular weight cases it was possible to fractionate and purify the diiodo intermediates by simple distillation. Brace also describes reactions between 1,3-butadiene and 1,6-heptadiene with iodoperfluorobutane; the butadiene reaction leads to an unstable product, and the heptadiene reaction is unusual in that cyclic reaction products predominate.[9]

In the case at hand, the overall synthetic approach as in Figure 1 is the same. However, with the larger perfluoroalkyl iodides ($n = 12$) and diolefins (particularly $m = 22$), the preparation of the triblock F*n*H*m*F*n*I2 intermediates and F*n*H*m*F*n* materials required some modifications in the methods that had previously been successfully used for the preparation of the diblock materials and the smaller triblock systems. It was impossible to distill any of the intermediates or products, and their general lack of solubility or unusual solubility made their overall preparation, purification, and subsequent characterization more difficult. The initial reaction between the per-

0024-9297/88/2221-1806$01.50/0

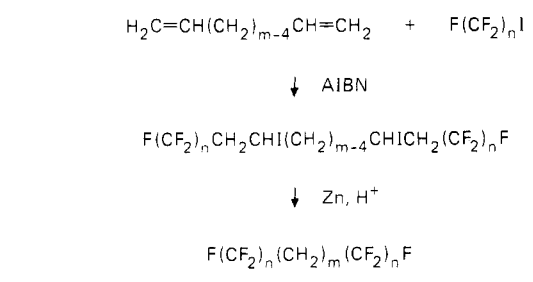

Figure 1. Synthetic scheme for F*n*H*m*F*n* molecules.

fluorododecyl iodide and the α,ω-diene was not modified significantly except that routine analysis of the progress of the reaction by gas chromatography was not possible. The dehalogenation reaction was particularly troublesome in that the intermediates were not soluble in boiling ethanol nor did they melt at the boiling point of ethanol (78 °C). Higher boiling alcohols including 1-propanol or 1-butanol were substituted and a cosolvent such as *n*-octane was introduced. Again, the progress of the dehalogenation reaction could not be easily followed by gas chromatography as in the case of the diblocks, and so large excesses of zinc and prolonged reaction times were employed to ensure complete reduction. Other reduction systems examined including zinc in acetic acid or zinc in pyridine were not found to be beneficial. Solvents for crystallization of the F*n*H*m*F*n*I2 and F*n*H*m*F*n* included 1,1,2,2-tetrachloroethane, perfluoro(dimethylcyclohexane), and most often perfluoro(butyltetrahydrofuran).

The triblock materials were characterized by melting point, Raman spectroscopy, combustion analysis, and proton NMR. The trends in the melting points and LAM-1 frequencies are as expected for the series of linear semifluorinated compounds with $2n + m$ varying between 30 and 46. The combustion analyses obtained for the F*n*H*m*F*n* compounds were often not in adequate agreement with the expected compositions. In some cases the total C, H, and F content was only about 98.5% of the sample, and the F content was always low in spite of multiple recrystallizations and determinations. The proton NMR spectra of these triblocks were difficult to obtain due to their insolubility in conventional solvents. Proton spectra were finally obtained at 100 °C in tetrachloroethane-1,2-d_2 but even here some unusual broadening of signals was found perhaps due to partially dissolved material. In the iodinated intermediates F*n*H*m*F*n*I2 the characteristic absorptions of of $R_FCH_2C\{H\}ICH_2-$ were at δ 4.38 (m, 1 H), of $R_FC\{H\}_2CHICH_2CH_2-$ were at δ 2.90 (d of m, 2 H), and of $R_FCH_2CHI_2C\{H\}_2-$ were at δ 1.87 (d of m, 2 H). In the F*n*H*m*F*n* no proton was found at δ 4.38, indicating complete loss of iodine; instead the absorption of protons $R_FC\{H\}_2CH_2CH_2-$ was at δ 2.10 (m, 2 H), the absorption of protons $R_FCH_2C\{H\}_2CH_2-$ was at δ 1.65, and the absorption of protons $R_FCH_2CH_2C\{H\}_2-$ was near δ 1.45 (m, 2 H). Any remaining aliphatic protons were not fully resolved and appeared at δ 1.27–1.43. In the particularly insoluble cases a broad absorption was also found at δ 2.2–3.4, and water appeared at δ 2.15.

More thorough studies will be required to optimize the preparations and purifications of these compounds, and other synthetic approaches will be required for the preparation of F*n*H*m*F*n* with $m < 6$. Typical reactions with 1,5-hexadiene and 1,21-docosadiene, which give the smallest and largest triblocks prepared, are provided.

Experimental Section

Characterization. Differential scanning calorimetric (DSC) measurements were made on a Dupont 1090 thermal analyzer. The melting temperatures tabulated in these studies correspond to the minimum of a DSC endotherm recorded at heating rates of 1–5 °C/min. In some cases, for F12H20F12 in particular, the melting was observed to be broad (>3 °C).

Proton magnetic resonance spectra were obtained on a Bruker AM-500 spectrometer. Internal lock was on deuterium in $CDCl_2CDCl_2$.

Raman measurements were made by using a Jobin-Yvon HG2S double monochromator equipped with the four-slit spatial filter configuration to increase stray light rejection. Excitation was provided by a Spectra Physics 165-08 argon ion laser operated at 488.0 nm. A thermoelectrically cooled RCA 31034A-02 photomultiplier tube was attached to the double monochromator and connected to standard photon-counting electronics. All data were processed and analyzed with a Nicolet 1180 data system. Unless otherwise noted all spectra were recorded at 2-cm^{-1} resolution by using a laser power of 150 mW and have not been either analogue or digitally filtered. High-temperature measurements were carried out by passing heated helium gas over the sample. The sample temperature was measured with an uncertainty of ±3 °C by using a thermistor placed 2–3 mm from the laser spot on the sample.

Synthesis. F12H6F12I2. 1,1,1,2,2,3,3,4,4,5,5,6,6,7,7,8,8,-9,9,10,10,11,11,12,12,19,19,20,20,21,21,22,22,23,23,24,24,25,25,-26,26,27,27,28,28,29,29,30,30,30-Pentadecafluoro-14,17-diiodotriacontane. Into a 200-mL pear flask with reflux condenser, stir bar, and nitrogen inlet were placed perfluorododecyl iodide (23.50 g, 31.5 mmol), *n*-octane (5 g), and 1,5-hexadiene (1.23 g, 15 mmol). The resulting mixture was warmed in a 90 °C oil bath, and AIBN was added through the condenser in portions (10 mg, 5×) over 15 min. The bath temperature was then raised to 125 °C, and more AIBN (10 mg, 5×) was again added over 15 min. The reaction was maintained at 125 °C for 15 min and then transferred to a 1-L flat-bottom flask with the aid of Freon TF (200 mL). The resulting slurry was boiled, more Freon TF was added (500 mL) until dissolution was almost complete, silica gel (about 5 g) was then added, and the solution was hot filtered. The filtrate was concentrated with stirring to about 200 mL, gradually cooled with stirring to room temperature, and then stirred in an ice bath. The white solid was isolated by suction filtration and washed with cold Freon TF to give 12.83 g of product. This material was further purified by two recrystallizations from 40 mL of perfluorotetrahydrofuran to give 12.35 g (52%) of product: mp 142 °C; ^{1}H NMR ($CDCl_2CDCl_2$) δ 1.99–2.20 (d, 4 H), 2.77–3.04 (d of m, 4 H), 4.37 (br s, 2 H).

F12H6F12. 1,1,1,2,2,3,3,4,4,5,5,6,6,7,7,8,8,9,9,10,10,11,11,-12,12,19,19,20,20,21,21,22,22,23,23,24,24,25,25,26,26,27,27,28,-28,29,29,30,30,30-Pentadecafluorotriacontane. Into a 1-L three-neck round-bottom flask with magnetic stirrer, condenser, bubbler, and HCl gas inlet were placed F12H6F12I2 (3.14 g, 2.0 mmol), *n*-octane (125 mL), and 1-butanol (125 mL). The resulting slurry became homogeneous prior to boiling, and HCl gas was admitted as the solution was maintained at a gentle boil. Zinc powder (6.54 g, 100 mmol, 25 equiv) was then added in small portions over the next 30 min, and the solution boiled an additional 30 min after completion of addition. The solution was gradually cooled to less than 100 °C; water (25 mL) was added and then cooled to room temperature with stirring. The resulting solid was isolated by suction filtration and washed with 1:1 butanol/water (50 mL). This solid was air dried on the filter, taken up in boiling Freon TF (250 mL) containing $MgSO_4$ and silica gel, and hot filtered. The filtrate was boiled down to 50 mL and diluted with acetone (50 mL) and refrigerated to give 2.26 g of crude product. This material was further purified by two consecutive crystallizations from perfluorodimethylcyclohexane (1.99 g, 75%): ^{1}H NMR ($CDCl_2CDCl_2$) δ 1.46–1.49 (m, 4 H), 1.65–1.69 (m, 4 H), 2.06–2.01 (m, 4 H). Anal. Calcd for $C_{30}H_{12}F_{50}$: C, 27.25; H, 0.91; F, 71.84. Found: C, 27.06; H, 0.86; F, 70.54.

F12H22F12I2. 1,1,1,2,2,3,3,4,4,5,5,6,6,7,7,8,8,9,9,10,10,11,-11,12,12,35,35,36,36,37,37,38,38,39,39,40,40,41,41,42,42,43,43,-44,44,45,45,46,46,46-Pentadecafluoro-14,33-diiodohexatetracontane. Into a 250-mL round-bottom flask with reflux condenser, stir bar, and nitrogen inlet were placed perfluorododecyl iodide (23.50 g, 31.5 mmol) and 1,21-docosadiene (4.60 g, 15 mmol). The resulting mixture was warmed in a 100 °C oil bath, and AIBN was added through the condenser in portions (25 mg, 5×) over 15 min and then maintained at 100 °C to give a homogeneous pink mixture. The reaction was then cooled and

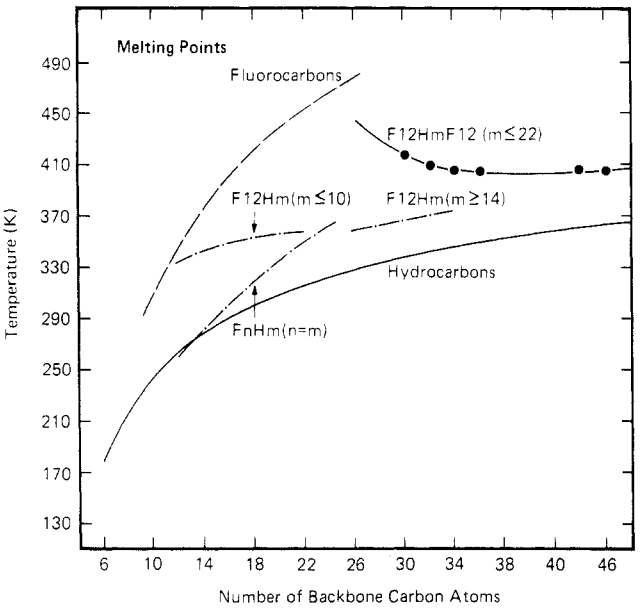

Figure 2. Plot of DSC-determined melting points for linear hydrocarbons, fluorocarbons, diblock semifluorinated molecules, F*n*H*m* ($n = m$), and F12H*m* ($m \leq 22$). Data points correspond to triblock F12H*m*F12 ($m \leq 22$). The heating rate for the latter was 10 °C/min.

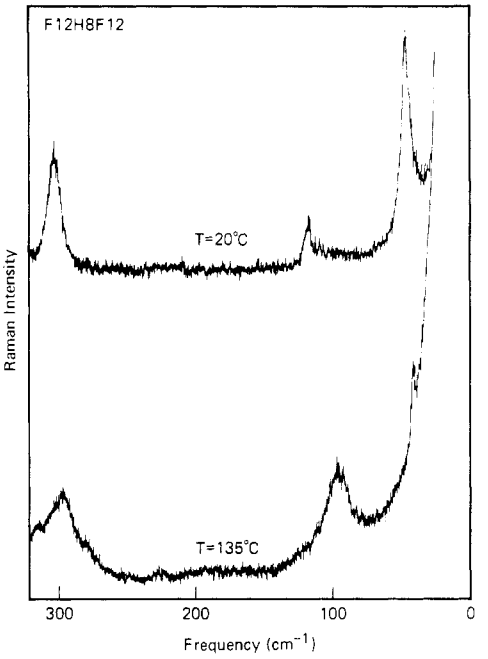

Figure 3. Low-frequency (30–330 cm^{-1}) Raman spectra of F12H8F12 obtained in both the melt and solid state. Approximately 150 mW of power (at 488.0 nm) was used to obtain these spectra at a resolution of 2 cm^{-1}. The sharp peak remaining at 39 cm^{-1} in melt spectrum is not a vibrational band but is due to a laser plasma line.

transferred to a 500-mL Erlenmeyer flask with the aid of Freon TF (300 mL). A small amount of silica gel and magnesium sulfate was added, and the resultant slurry boiled and hot filtered. As the Freon TF was boiled away, it was replaced by acetone until only 200 mL remained. The slurry was cooled and filtered, and the white solid washed well with acetone and finally recrystallized twice from 75 mL of perfluoro(butyltetrahydrofuran) to give 20.99 g (79%) of product: mp 110 °C (also present was a smaller endotherm at 103 °C, which might be due to contamination by monoadduct $C_{34}H_{42}F_{25}I$); ^1H NMR ($CDCl_2CDCl_2$) δ 1.28–1.56 (m, 32 H), 1.78–1.93 (d of m, 4 H), 2.79–2.98 (d of m, 4 H), 4.34–4.39 (m, 2 H) (also present were resonances due to apparent contamination by the monoadduct $C_{34}H_{42}F_{25}I$, 2.07–2.05 (dd), 4.95–5.04 (dd), and 5.85–5.91 (dd)).

F12H22F12. 1,1,1,2,2,3,3,4,4,5,5,6,6,7,7,8,8,9,9,10,10,11,11,-12,12,35,35,36,36,37,37,38,38,39,39,40,40,41,41,42,42,43,43,44,44,-45,45,46,46,46-Pentadecafluorohexatetracontane. Into a 1-L three-neck round-bottom flask with stir gas, gas inlet, condensor, and bubbler were placed the F12H22F12I2 (5.28 g, 3.0 mmol) and 1-propanol (150 mL). The resulting slurry was brought to a gentle boil, and *n*-octane was added until the solution became homogeneous (50 mL). To this boiling solution HCl gas was admitted, and then zinc powder (9.81 g, 150 mmol) was added in portions (gas evolution and foaming) over the next 90 min. After zinc addition was complete, the slurry was boiled 30 min more, water (10 mL) was added, and the solution was cooled with stirring. The crude solid product was isolated by suction filtration, washed with 1:1 MeOH/water, and air dried. The crude product was taken up in boiling perfluorotetrahydrofuran (200 mL) with some silica gel and magnesium sulfate and hot filtered. The product was isolated by filtration (3.65 g), and this material was recrystallized again in the same fashion, to yield 3.21 g (71%) of product: ^1H NMR($CDCl_2CDCl_2$) δ 1.27–1.44 (m, 36 H), 1.63–1.66 (m, 4 H), 2.08–2.14 (m, 4 H). Anal. Calcd for $C_{46}H_{44}F_{50}$: C, 35.72; H, 2.87; F, 61.41. Found: C, 36.98, H 3.16; F, 58.31.

Results and Discussion

Thermal Analysis. Differential scanning calorimetric (DSC) measurements were carried out on the triblocks, F*n*H*m*F*n*, and the resulting melting points are shown in Figure 2, where they are plotted as a function of the total number ($2n + m$) of backbone carbon atoms. Also shown for comparison are curves of two other series of oligomers F*n*H*m* ($m = n$) and F12H*m* ($0 \leq m < 22$), whose melting points have been previously determined. Of particular interest are the melting curves for the fluorocarbons[10] and hydrocarbons[11] since they represent the limiting behavior of the melting points for the F12H*m*F12 triblock materials. For the triblocks, as m increases the melting point curve is approaching (or at least running parallel to) that of the hydrocarbons. Since in the F12H*m*F12 molecules the fluorocarbon sequences remain fixed in length, then as m increases to large values the effect of the fluorocarbon end groups on the overall energetics of packing into a lattice will be increasingly diminished. Hence, at very large m values the melting points should eventually coincide with those of the hydrocarbons since the effect of the end groups becomes negligible.

At the other extreme (small m values) the melting curve of the F12H*m*F12 molecules reveal an interesting insight into the melting points of perfluorinated *n*-alkanes. As shown in Figure 2, at short hydrocarbon sequences (low m values) the F12H*m*F12 curve undergoes a change in slope toward higher melting points. The intersection of this curve with the fluorocarbon melting curve occurs at an abscissa value of 24 backbone atoms, corresponding to $m = 0$ in the F12H*m*F12 series. This would predict that the melting point of the fluorocarbon, $F(CF_2)_{24}F$, would be 463 K. Interestingly enough, at the time of these measurements, fluorocarbon molecules with greater than 20 backbone atoms were not available, and hence no information regarding melting points was available in the literature. In contrast, melting points for *n*-paraffins have been available for over 25 years.[11] However, very recently, Starkweather[12] successfully synthesized and purified a sample of $F(CF_2)_{26}F$ and reported its melting point to be 465 K, in excellent agreement with that obtained for our extrapolation of the melting point data for the F12H*m*F12 materials. F*n*H*m*F*n* with $0 < m < 6$ have not yet been prepared, so this interesting convergence in melting points remains to be studied in detail.

Raman Measurements. Low-frequency (30–330 cm^{-1}) Raman spectra of a typical triblock semifluorinated *n*-alkane, F12H8F12, are shown in Figure 3 at both ambient

Table I
Observed LAM Frequencies for FnHmFn Triblock Copolymers

compound	Raman frequency, cm^{-1} solid LAM-1	solid LAM-3	melt
F12H6F12	42	116	95.5
F12H8F12	40	112	94.7
F12H10F12	37	109	93.5
F12H12F12	35	105	93.0
F12H20F12	32	101	93.5
F12H22F12	30	100	93.2

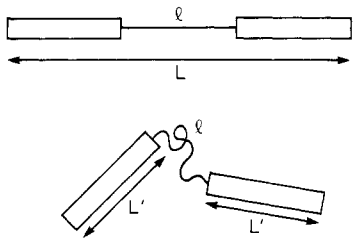

Figure 4. Schematic representation of molecular topography of F12HmF12 in the solid (top) and melt (bottom) state. The rectangular portion represents the F12 segment, while the line indicates the hydrocarbon sequence: L, extended molecular length; l, length of hydrocarbon sequence; L', length of helical fluorocarbon sequence.

temperature and in the melt state at 135 °C. A number of spectroscopic changes occurr as the material goes from the solid state to the melt. At room temperature, three bands of moderate intensity are observed. The most intense at 40 cm^{-1} can be assigned to the Raman-active LAM-1. The weaker band found at 112 cm^{-1} can most reasonably be assigned to the multinodal vibration LAM-3, although its intensity is somewhat larger than would be expected from similar studies on n-alkanes.[13] The medium band at 295 cm^{-1} has been previously[14-16] assigned to a CF_2 bending vibration in ordered fluorocarbon sequences.

Substantial changes occur in the bands assigned to LAM-1 and LAM-3 upon heating the F12H8F12 above its melting point. Both disappear and are replaced by a broad band at 95 cm^{-1}. This position is very close to that (96 cm^{-1}) found for LAM-1 in $F(CF_2)_{12}F$ in the solid state.[4] Similar results were found for the entire series of F12HmF12 compounds as shown in Table I. In all cases, although the position of LAM-1 and LAM-3 bands differ considerably for each of the triblock copolymers in the solid state, the position of the single broad band in the melt spectrum is always found in the vicinity of 94 cm^{-1}. A reasonable explanation for this observed behavior is shown schematically in Figure 4. In the solid state, the observed LAM-1 and LAM-3 frequencies can be attributed to the longitudinal oscillations of the entire extended molecule of length L. This would then suggest that as the length of the F12HmF12 moleucles increases (larger m values), the frequencies of the LAM-1 and LAM-3 vibrations should decrease as expected from the frequency/inverse chain length relationship observed for LAM. As shown in Table I, this is exactly what is observed. For example, LAM-1 varies from 42 cm^{-1} found for F12H6F12 to 30 cm^{-1} observed for F12H22F12. This fact is graphically illustrated in Figure 5, where the frequency of LAM-1 in the solid state is plotted versus the inverse of the total number of backbone carbon atoms. For comparison, also plotted in this figure are similar data for the LAM-1 frequencies of both a series of hydrocarbon and fluorocarbon oligomers. Interestingly enough there is a deviation from the fluorocarbon curve that increases at large values of m, i.e., at long

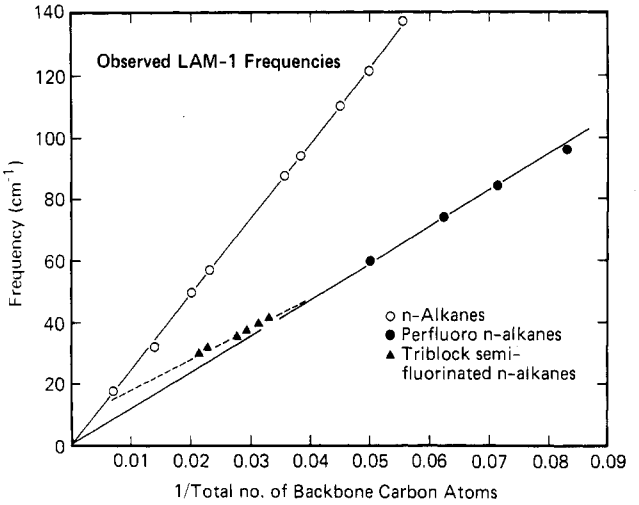

Figure 5. Plot of observed LAM-1 frequency of triblocks versus total number of backbone carbon atoms ($2n + m$). Data for fluorocarbon and hydrocarbon oligomers are included for reference.

hydrocarbon lengths for the F12HmF12 materials. This is thought to reflect the fact that at low m values the F12HmF12 compounds are essentially fluorocarbons and as such undergo a LAM-1 vibration characteristic of the helical conformation adopted by these molecules. On the other hand at large m values (long hydrocarbon lengths), the LAM-1 vibration of the F12HmF12 molecules begins to reflect the LAM-1 of the planar zigzag hydrocarbon portion of the molecule, and hence the frequencies begin to move toward those of the hydrocarbon curve. At infinitely large values of m, the LAM-1 frequencies of the F12HmF12 molecules would be expected to be coincident with those of the hydrocarbons, since the length of the fluorocarbon "end groups" would be negligible compared to the length of the planar zigzag portion.

An explanation of the observations in the melt state is a bit more complex. Qualitatively the replacement of LAM-1 and LAM-3 by a single band in the region of 94 cm^{-1} can be understood by reference to the lower portion of Figure 4. As the F12HmF12 compounds enter the liquid state, the central hydrocarbon part will most certainly disorder due to the fact that the planar zigzag conformation in the solid state is primarily due to intermolecular interactions in the lattice.[7] Once those constraints are removed, the introduction of gauche bonds in this part of the molecule is facilitated, thus leading to random disorder.

The F12 components, on the other hand, have been shown previously to retain their rodlike shape in the melt[4,10] since their helical conformation is stabilized by intramolecular steric effects. Although it is possible that defects such as helix reversals can be introduced[17] at elevated temperatures, these defects have been shown to preserve the axial nature of the molecule[16] and, as such, do not influence the LAM-1 frequency of the F12 segment. Hence the molecular picture in the melt state is illustrated in the lower part of Figure 4. The connective hydrocarbon segment of length l becomes randomly disordered above the melting point, interrupting the extension of the F12HmF12 molecule. Thus, the observed LAM-1 frequency results from the longitudinal oscillations of the fluorocarbon segments of length L'. The slight perturbation in frequency from that of the $F(CF_2)_{12}F$ molecule is due to the fact that the rod of length L' is not oscillating as a rod with free ends[4,5] since it is attached to the F12Hm segment. This observation was first made in a series of diblock copolymers,[4] FnHm, and was attributed to the fact

Table II
Valence Force Constant Values[a] Used for the Calculation of Low-Frequency Motions in F12H*m*F12 Molecules

force constant	value
CC stretch	3.963 mdyn/Å
CCC bend	0.942 mdyn/Å
CC,CC stretch–stretch interaction	0.148 mdyn/Å
CCC,CCC bend–bend interaction	0.492 mdyn Å
CC,CCC stretch–bend interaction	0.166 mdyn

[a] From ref 19.

that a slight perturbation of the LAM-1 frequency of the F12 rod is caused by the first three–four bonds of the attached hydrocarbon molecule. An analogous effect appears to occur in the melt of the F12H*m*F12 molecules as seen in Table I. When there are six or eight CH_2 groups in the connecting link between the two rods of length L' in the melt, there is a slight perturbation of the LAM-1 frequency. Whem m becomes 10 or larger, no further effect on the frequency is observed. One can conclude that the origin of this effect is due to the small amount of coupling that may still result in the melt from short segments of length l (see Figure 4). As the length increases, this coupling disappears, and no further perturbation of the LAM-1 frequency occurs.

Normal Coordinate Analysis. Normal coordinate analyses were undertaken to further understand the nature of the LAM in both diblock and triblock semifluorinated *n*-alkanes in the solid state. A 15/7 helical conformation for the F12 segment was assumed on the basis of the room-temperature structure of poly(tetrafluoroethylene).[18] For comparison, a planar zigzag conformation of the fluorocarbon segment was also considered.

In all cases an isolated chain in the skeletal approximation was used. Thus the CF_2 and CH_2 groups were treated as point masses, i.e., they were considered as single atoms having masses of 50 and 14 amu, respectively. Previous studies on a series of *n*-paraffins[19] have shown that this approximation has only minor effects on the actual calculated LAM frequency. A similar valence force field[20,21] defined for an ethylene–tetrafluoroethylene copolymer including CC stretching, CCC bending, and CC torsional force constants and their nearest-neighbor interactions was used for both hydrocarbon and fluorocarbon parts of the molecule considered in this study. Force constant values, transferred from previously published results,[20] are listed in Table II.

It is also instructive to plot the Cartesian displacements of each atom corresponding to a LAM vibration since the effect of a perturbation can easily be assessed by studying atomic motions. One such example is shown in Figure 6, where the longitudinal atomic displacements for LAM-1 are plotted in both a diblock (F18H18) and a triblock (F12H12F12) semifluorinated *n*-alkane. Several interesting observations can be made. In the F18H18 molecule neither the calculated frequency nor the atomic displacements for LAM-1 were affected by the conformation of the fluorocarbon segment, i.e., assuming either a helical or a planar zigzag conformation for the F18 segment caused no change in the calculated frequency or atomic displacements. More importantly, as shown in Figure 6, a displacement of the node in atomic motion for LAM-1 was observed. Instead of being located at the chain center as is usually the case, the node in atomic displacement is shifted into the fluorocarbon portion of the molecule. This observation has also been observed by Minoni and Zerbi[5] for a series of varying length diblock semifluorinated *n*-alkanes. In contrast, the mass-weighted Cartesian displacements for a symmetric triblock molecule (F12H12F12) are shown in

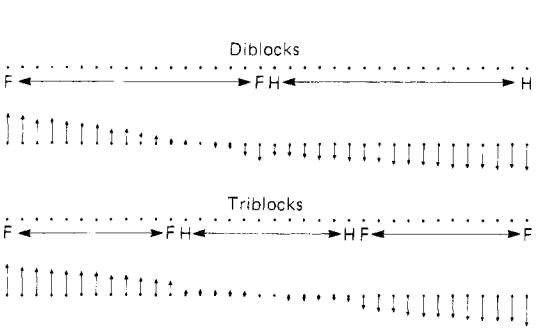

Figure 6. Longitudinal atomic displacements (plotted vertically) of backbone carbon atoms for LAM-1 in both diblock and triblock semifluorinated *n*-alkanes. F and H indicate length of fluorocarbon and hydrocarbon sequences in each molecule.

Table III
Comparison of Observed and Calculated Values (cm^{-1}) of LAM for F12H*m*F12 Molecules in the Solid State

	LAM-1		LAM-3	
F12H*m*F12	exptl	calcd	exptl	calcd
F12H6F12	42	39	116	121
F12H8F12	40	37	112	116
F12H10F12	37	35	109	112
F12H12F12	35	33	105	109
F12H20F12	32	27	101	101
F12H22F12	30	27	100	99

the lower part of Figure 6. Clearly the node of LAM-1 is located at the center of the molecule since it is symmetrically weighted and contains the same number of CH_2 and CF_2 groups on both sides of the center.

Surprisingly enough, even with the skeletal and point mass approximations, there is a reasonable agreement between calculated and observed LAM values for the triblock molecules as shown in Table III. More importantly is the calculated change in relative frequency as the chain length changes. For LAM-1 a change of 12 cm^{-1} is predicted in going from F12H22F12 to F12H6F12. This is an excellent agreement with the observed change of 12 cm^{-1}. Likewise, a frequency difference of 22 cm^{-1} is predicted for LAM-3, compared with 16 cm^{-1} actually observed. Thus it appears as if the approximations made previously are justified since the calculated and observed values of LAM-1 and LAM-3 follow the same trends, as expected.

Of equal importance is the atomic displacements of the triblock molecule during the LAM-1 vibration shown in Figure 6. It is clear that no decoupling of the longitudinal motion occurs at the juncture of the fluorocarbon portions of the molecule. However, as shown, the atomic displacements of the CH_2 and CF_2 groups are different due to the fact that these normal modes were calculated by using mass-weighted Cartesian displacement coordinates. Taking this fact into consideration, it is apparent that during the LAM-1 vibration the entire extended molecule undergoes lontitudinal motion.

Conclusion

Thermal studies of a series of F12H*m*F12 compounds have revealed a single endotherm above room temperature attributable to a crystalline melting point. Extrapolation of these points to $m = 0$ (corresponding to $F(CF_2)_{24}F$) gives a value of 463 K for the melting point of the corresponding fluorocarbon, compared to a value of 465 K recently reported.[12]

The spectroscopic results of this work have shown conclusively that a LAM vibration does exist in triblock sem-

ifluorinated *n*-alkanes in the solid state and that, furthermore, its vibrational frequency is characteristic of the entire extended molecule. Thus no decoupling of the chain vibration occurs at the juncture between the helical and planar zigzag conformations.

In the melt state, however, the molecular picture is quite different. A disordering of the hydrocarbon segment of the F12H*m*F12 molecule occurs at the melting point, effectively decoupling the longitudinal oscillations of F12 segments. Hence the observed Raman frequency reflects the LAM of the much shorter F12 segment. At short lengths (small *m* values) of the disordered hydrocarbon, the LAM frequency of the F12 segment is perturbed due to a slight coupling with the other attached F12 segment. When this length exceeds 10 CH_2 groups, there is no further perturbation on the LAM frequency.

Acknowledgment. J.F.R. acknowledges partial support of this work by the NSF Division of Materials Research. We acknowledge the assistance of R. L. Siemens in obtaining the thermal measurements and W. Fleming, C. Wade, and C. Gettinger for the NMR determinations.

Registry No. $F_{12}H_6F_{12}$, 114221-77-1; $F_{12}H_8F_{12}$, 100550-09-2; $F_{12}H_{10}F_{12}$, 100550-10-5; $F_{12}H_{12}F_{12}$, 100550-11-6; $F_{12}H_{20}F_{12}$, 114221-78-2; $F_{12}H_{22}F_{12}$, 114221-79-3; $F_{12}H_6F_{12}I_2$, 114221-75-9; $F_{12}H_{22}F_{12}I_2$, 114221-76-0; $F(CF_2)_{12}I$, 307-60-8; $H_2C{=}CH(CH_2)_2CH{=}CH_2$, 592-42-7; $H_2C{=}CH(CH_2)_{18}CH{=}CH_2$, 53057-53-7; $F(CF_2)_{24}F$, 1766-41-2.

References and Notes

(1) Mizushima, S. I.; Shimanouchi, T. *J. Am. Chem. Soc.* **1949**, *71*, 1320.
(2) Peticolas, W. L.; Hibler, G. W.; Lippert, J. L.; Peterlin, A.; Olf, H. *Appl. Phys. Lett.* **1971**, *18*, 87.
(3) Rabolt, J. F. *CRC Crit. Rev. Solid State Mater. Sci.* **1985**, *12*, 165.
(4) Twieg, R. J.; Rabolt, J. F. *J. Polym. Sci., Polym. Phys. Ed.* **1983**, *21*, 901.
(5) Minoni, G.; Zerbi, G. *J. Polym. Sci., Polym. Lett. Ed.* **1984**, *22*, 533.
(6) Rabolt, J. F.; Russell, T. P.; Twieg, R. J. *Macromolecules* **1984**, *17*, 2786.
(7) Russell, T. P.; Rabolt, J. F.; Twieg, R. J.; Siemens, R. L.; Farmer, B. L. *Macromolecules* **1986**, *19*, 1135.
(8) Brace, N. O. *J. Am. Chem. Soc.* **1964**, *86*, 523.
(9) Brace, N. O. *J. Org. Chem.* **1966**, *31*, 2879.
(10) Rabolt, J. F.; Fanconi, B. *Polymer* **1977**, *18*, 1258.
(11) Broadhurst, M. G. *J. Res. Natl. Bur. Stand. Sect. A* **1962**, *66A*, 241.
(12) Starkweather, H. *Macromolecules* **1986**, *19*, 1131.
(13) Olf, H. G.; Fanconi, B. *J. Chem. Phys.* **1973**, *59*, 534.
(14) Hannon, M. J.; Boerio, F. J.; Koenig, J. L. *J. Chem. Phys.* **1969**, *50*, 2829.
(15) Masetti, G.; Cabassi, F.; Morelli, G.; Zerbi, G. *Macromolecules* **1973**, *6*, 700.
(16) Rabolt, J. F.; Fanconi, B. *Macromolecules* **1978**, *11*, 740.
(17) Clark, E. S. *J. Macromol. Sci., Phys.* **1967**, *B1*, 795.
(18) Bunn, C. W.; Howells, E. R. *Nature (London)* **1954**, *174*, 549.
(19) Shimanouchi, T.; Tasumi, M. *Indian J. Pure Appl. Phys.* **1971**, *9*, 958.
(20) Kobayashi, M.; Tashiro, K.; Tadokoro, H. *Macromolecules* **1975**, *8*, 158.
(21) Zabel, K.; Schlotter, N. E.; Rabolt, J. F. *Macromolecules* **1983**, *16*, 446.

Effect of Plasticization on Mass Diffusion of Camphorquinone in Polystyrene

J. Zhang and C. H. Wang*

Department of Chemistry, University of Utah, Salt Lake City, Utah 84112.
Received May 15, 1987; Revised Manuscript Received November 13, 1987

ABSTRACT: Mass diffusion coefficients of camphorquinone (CQP) in the polystyrene–dioctyl phthalate (plasticizer) system are measured at various temperatures and concentrations of dioctyl phthalate (DOP) by using the laser-induced holographic grating relaxation technique. The mass diffusion coefficient of CQP shows a strong dependence on the concentration of DOP, which is explained in terms of the free volume increase introduced by the plasticizer. At a given temperature, the diffusion coefficient of CQP in polystyrene (PS) containing 12.4% of DOP is more than 10^4 times higher than that in pure PS. The apparent activation energy is found decreasing as the plasticizer concentration increases.

Introduction

The study of the diffusion process of small molecules in macromolecular matrices is fundamental to the basic understanding of the diffusion mechanism and many operations of polymer processing. It is of key importance to many diffusion-controlled processes such as permeation, diffusion-controlled chemical reactions, and controlled drug delivery. In these processes, it is desirable to control, either to increase or to decrease, the diffusion rate. One of the ways to accomplish this is by altering the polymer matrices. In our previous work, we have reported reducing the diffusion coefficient by forming cross-links in the polymer hosts.[1,2] In this study, we report increasing the diffusion rate by plasticizing the polymer host. Plasticization is the process in which the plasticizer molecules neutralize secondary valence bonds or van der Waals force between polymer molecules. It then increases the chain mobility and the fractional free volume of the polymer. As a result, it reduces moduli or stiffness, increases the ability for elongation and chain flexibility, and lowers the glass transition temperature of the polymer.

Since plasticization increases the chain mobility and fractional free volume of the polymer,[3] we expect the diffusion rate of the probe molecule to increase. It is the objective of this work to carry out a quantitative study of the dependence of the diffusion coefficient on the degree of plasticization and temperature of the plasticized polymer. The plasticizer used is dioctyl phthalate (DOP), a member of the most important plasticizer family. It is an external plasticizer that interacts with the polymer without undergoing the chemical reaction. The organic diffusant and the polymer used are camphorquinone (CQ) and polystyrene (PS), respectively.

In the vicinity of the glass transition temperature of PS, the diffusion coefficient of CQ is in the range of 10^{-14}–10^{-10} cm^2/s, depending on the plasticizer concentration and the

0024-9297/88/2221-1811$01.50/0